

# Height estimation of pine (*Pinus eldarica*) single trees using slope corrected shadow length on unmanned aerial vehicle (UAV) imagery in a plantation forest

Ali Hosingholizade<sup>1</sup>, Yousef Erfanifard<sup>1</sup>✉, Seyed Kazem Alavipanah<sup>1</sup>, Hooman Latifi<sup>2</sup>, Yaser Jouybari-Moghaddam<sup>3</sup>

**Hosingholizade A., Erfanifard Y., Alavipanah S.K., Latifi H., Jouybari-Moghaddam Y., 2023.** Height estimation of pine (*Pinus eldarica*) single trees using slope corrected shadow length on unmanned aerial vehicle (UAV) imagery in a plantation forest . Ann. For. Res. 66(2): 3-16.

**Abstract** Tree height is one of the key parameters in forest plantations that plays a crucial role in estimation of above-ground biomass (AGB) of trees and stands. The parameter may be obtained by different methods from airborne remotely sensed datasets such shadow length of each tree individual or crown height models (CHMs). However, tree height estimation based on shadow length might be biased considering diverse topography of forest sites. Therefore, this study aims to develop a reliable method to estimate tree height in a plantation forest using shadow length on UAV imagery. First, heights of 151 pine (*Pinus eldarica*) trees were precisely measured in Pardisan Park, North Khorasan province, Iran. Additionally, a collection of images was captured by a Phantom 4Pro UAV in order to illustrate the study area. Then, two different approaches were considered to estimate the height of trees. In the first approach, tree heights were estimated based on shadow length on the UAV orthomosaic and correcting the effect of slope. The second approach considered the UAV-based CHM and height estimation using CHM segmentation and local maximum filtering. The results showed that tree heights estimated by the first approach were not significantly different from the in-situ data ( $p=0.298$ ). Furthermore, the heights estimated by the slope corrected shadow length showed higher precision compared to the heights estimated by the shadow length without slope correction (Relative root mean squared error, RRMSE 5.6% and 8.2% respectively). However, the heights obtained from the first approach were less precise than the second approach (RRMSE 5.6% and 4.2% respectively). In general, it was concluded that height estimation of pine trees based on shadow length after correction of slope effects can be considered as a reliable approach, although CHM is more efficient in estimating the tree heights. The findings of this study are applicable for height estimation of pine trees within plantation forests on UAV imagery.

**Keywords:** Tree shadow, CHM, segmentation, slope correction.

**Addresses:** <sup>1</sup>Dept. of Remote Sensing and GIS, Faculty of Geography, University of Tehran, Tehran, Iran. | <sup>2</sup>Dept. of Photogrammetry and Remote Sensing, Faculty of Geodesy and Geomatics Engineering, K.N. Toosi University of Technology, Tehran, Iran | <sup>3</sup>Dept. of Surveying Engineering, Faculty of Engineering, University of Bojnord, Bojnord, Iran.

✉ **Corresponding Author:** Yousef Erfanifard (erfanifard@ut.ac.ir)

**Manuscript:** received June, 20, 2023; revised September 26, 2023; accepted September 28, 2023.

## Introduction

Plantation forests are man-made forests that provide valuable commercial, recreational and environmental services that are helpful in reducing pressure on natural forests and preserving significant species (Navarro et al. 2020, Zhu et al. 2020). Additionally, these forests play a crucial role in reducing global climate change and its effects, maintaining biodiversity, water and soil resources (Suzuki et al. 2006, Zhou & Zhang 2020). According to the recent report of the Food and Agriculture Organization of the United Nations (FAO), the worldwide area of plantation forests is 292 million hectares in 2020, of which almost one million hectares of them are located in Iran (FAO, 2020). Considering the important roles of plantation forests and the ever-increasing development of their extent, their effective management has now become more imperative than in the past, and requires access to quantitative and qualitative information. This information helps managers and planners in formulating policies and plans. One of the required pieces of information is accurate and effective measurements of quantitative parameters such as height and diameter at breast height (DBH), especially at single tree levels (Thu Moe & Owari 2020).

One of the quantitative characteristics of trees is total height, which is very important from various aspects such as estimating above-ground biomass (AGB) in plantation forests. Furthermore, tree height is important for ecological and commercial reasons, and indicates the production capacity of habitat of critical species (Grote et al. 2016, Krause et al. 2019). Tree height is also a key parameter for calculating growth, volume and soil fertility (Guo et al. 2021, Kargar & Sohrabi 2019) and plays a crucial role in evaluating the economic value of a plantation forest stands (Moe et al. 2020). Monitoring tree height dynamics on monthly and annual temporal scales is important for the calibration and validation of

growth models (Dempewolf et al. 2017, Puliti et al. 2020), management and studies of forest ecology and biophysical processes (Onishi & Ise 2021, Onishi et al. 2022). Accurate assessment of tree height might improve modeling efficiency of biophysical properties at single tree- and stand levels (Dempewolf et al. 2017).

In general, there are direct and indirect methods for tree height measurement (Tian et al. 2019, Hartley et al. 2020). In direct measurement of tree height, tools such as forester's stick (Gyawali et al. 2022) and total station mapping cameras (Yao et al. 2022) are common. In indirect measurements, methods such as allometric equations (Barbosa et al. 2019) and application of shadow length and trigonometric relationships on remote sensing data are frequently used in the literature (Safonova et al. 2021). Despite diverse available field methods, direct in-situ measurement of tree height is associated with difficulties in addition to cost and time consumption. Overall, accuracy and precision of field-based height measurements are significantly influenced by direct vision of top of a tree which needs multiple displacements to find an appropriate location of a landmark and necessity of in-person reference (Bragg, 2014, Apostol et al. 2016). Therefore, it seems necessary to have access to methods that can determine height of trees quickly, accurately and cheaply. Additionally, such methods are essential in plantation forests since forest managers tend to access quantitative information at single tree levels.

An increased accessibility to images with very high spatial resolution (VHR) now exists along with the rapid development of remote sensing instruments such as satellites, digital sensors and cameras such as UltraCam and Unmanned aerial vehicles (UAV) cameras. Compared to images with medium and low spatial resolutions, VHR images have a greater ability to reveal terrestrial phenomena with more details, thus these images have

been widely used in quantitative assessment of natural and plantation forests (Kislov *et al.* 2020), particularly over small spatial scales. UAVs are amongst the common cost-effective platforms used by both scientists and managers in the last decade (Chadwick *et al.* 2020, Vélez *et al.* 2022a). Considering the overlapping of sequential UAV images, point clouds with different point densities can be obtained from the images. A Digital Surface Model (DSM) and a Digital Terrain Model (DTM) can be consequently produced by classification of points into ground and non-ground points. The subtraction of DSM and DTM results in Crown Height Model (CHM). The efficiency of CHM in estimating the height of single trees has been confirmed in different ecosystems including coniferous forests (Paneque-Gálvez *et al.* 2014, Gülcü 2019). However, point clouds with high point density and the resulting CHM are not available in all VHR remote sensing datasets such as VHR satellite images, as it may not be possible to use CHM for tree height estimation. Furthermore, point clouds produced from RGB images might significantly be influenced by different parameters such as quality of camera, overlapping rate of sequential images, limitation of software and algorithms. CHMs constructed based on such point clouds are not applicable to height estimation within all forest ecosystems as previous studies (Erfanifard *et al.* 2019, Selim *et al.* 2020; Safonova *et al.* 2021) measured tree heights on UAV images. Therefore, it is necessary to develop methods that can be directly used on VHR images obtained from airborne platforms such as UVAs.

Shadow length on RGB images has been successfully used to estimate height of single trees in the literature. For instance, Safonova *et al.* (2021) also estimated the height of olive trees in southern Spain using shadow length on color UAV images. Selim *et al.* (2020) measured the height of urban trees with shadow length on UAV images in Antalya, Turkey. Furthermore, Rezayan and Erfanifard (2016) modeled the height of coppice oak trees in a part of the Zagros

oak forests of in western Iran using shadow length on UltraCam aerial images. Application of shadow length on VHR imagery such as UAV images in estimating height of single trees has been confirmed in previous studies in almost flat areas, although it has been less noticed that accuracy and precision of tree height estimation using shadow length may be influenced by topography in mountainous areas. Therefore, it is necessary to consider slope of tree location as it leads in extending its shadow and potentially affects tree height measurement using shadow length. Otherwise, height of trees based on shadow length may be over- or underestimated compared to the true values.

In line with previous studies, our research evaluates the efficiency of shadow length on VHR images in height estimation of single trees in a plantation forest. Theoretically, length of tree shadows is influenced by the terrain topography so that for a tree with a certain height, the length of shadow is longer on downward slopes. However, on upward slopes the shadow length appears shorter than it should be. Correction of slope effects on shadow length may improve the accuracy of height estimation on remotely sensed data. Therefore, the main goal of this study is to investigate the effect of the slope on height estimation of single trees using shadow length on UAV-based VHR images. In addition, the height obtained by correcting the effect of slope on the shadow length is compared with the height obtained from CHM and the true height value obtained from the field data. The findings of this study will show how accurate it is to estimate tree height on VHR RGB images and will reveal if it is necessary to correct the effect of slope on shadow length in measuring height of trees in mountainous plantation forests.

## Materials and Methods

### Study area

The study area is located in a part of Pardisan Park in the east of Bojnord city in North

Khorasan province in northeastern Iran ( $37^{\circ} 57' 28''$  N and  $57^{\circ} 49' 25''$  E). The region is cold and semi-arid based on Köppen's climate classification (Roshani et al. 2021) and has lowlands and relatively high elevation changes with a general east-west slope and an average height of 1080 m above sea level. The area is covered by pine trees (*P. eldarica* (Medw.) Silba, syn. *P. brutia* Ten. var. *eldarica* Medw.) with a distance of approximately 3 m, which were planted in 2004 and 2010. The 6-year interval between the plantations has brought variety in size of trees. According to the meteorological statistics of Bojnord Airport station (the closest station to the studied area) in a period of 10 years (2011-2021), the air temperature fluctuates from a minimum of  $-10^{\circ}\text{C}$  in the middle of January to a maximum of  $42^{\circ}\text{C}$  in August. The average annual rainfall of the region is 260 mm and the average annual temperature is  $15^{\circ}\text{C}$ .

area showed that the topography has many slopes and the range of elevation changes is from 1036.5 to 1111.9 m (Fig. 1).

According to the objectives of the research, all 151 pine trees spatially distributed on gentle and steep slopes in the study area were recorded and their heights were measured within five days of field work. The selected pine trees were from different DBH classes to reliably test the hypotheses of the present study. The spatial locations of single trees were first recorded using Raymand iRoG3B dual-frequency global positioning system under the National Shamim System (proprietary integrated positioning network) with a planar accuracy of 0.45 cm and a height accuracy of 0.80 cm. In order to correctly and uniformly map trees in the range of planar and height accuracies, the allowed range of accuracy (planar accuracy less than 0.50 cm and height

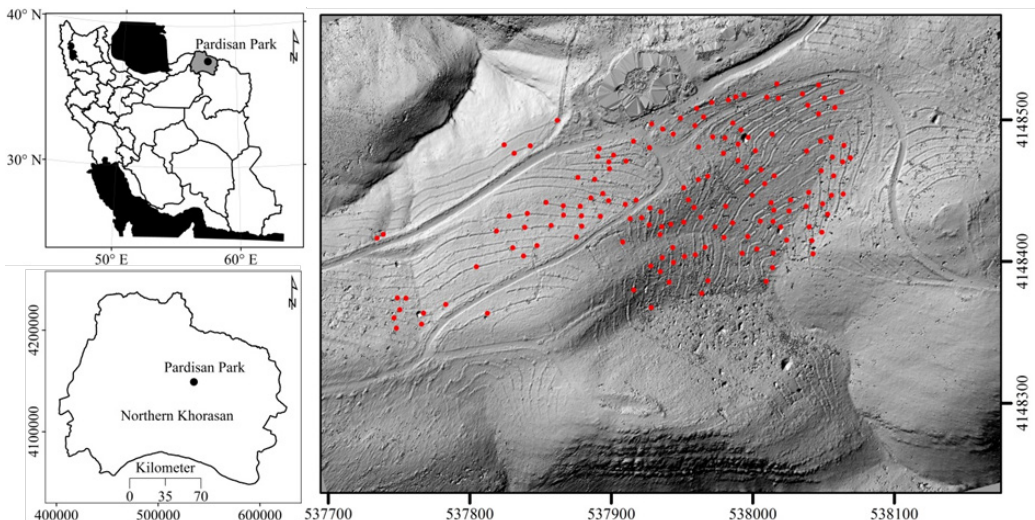


**Figure 1** The location of 151 pine trees (red dots) on the Digital Terrain Model (DTM) with a spatial resolution of 2 cm in a part of Pardisan Park (black dot), North Khorasan province (grey polygon), Iran.

### ***In-situ* data collection**

Although the area of the park is about 351 ha, from which approximately 21 ha is covered by plantation stands of pure pine trees. Due to the restrictions in issuing permits for the UAV flight in the region, only 14 ha were surveyed. The Digital Terrain Model (DTM) of the study

accuracy less than 1.0 cm) was defined in the used device to record the position of the tree outside the defined range. Additionally, by activating the tilt sensor of the device, the correct position of each tree was carefully recorded so that any human error caused by the device not being leveled by the operator at the time of observation was removed. Then

the heights of the trees were measured with a Leica TS02 total station camera with a nominal accuracy of 7 seconds and recorded in the sampling forms considered as the ground truth in this study.

**Aerial data collection**

Phantom 4 Pro UAV was used to collect imagery at the study site. The UAV has a three-axis gimbal to prevent any vibration and create a proper balance of the camera in different image capture missions in a way that prevents the capture of images with a lot of tilt. In this study, the images were collected according to the type of topography at a height of 40 m (Seifert *et al.* 2019) and vertically with a longitudinal and transverse overlap of 80 and 40 percent (Dandois *et al.* 2015, Surový *et al.* 2018). All images were then visually checked for blurring and light scattering at image edges. In addition, gentle wind with a speed of less than one knot and clear weather were considered in the selection of the flight day. The general specifications of the camera used and the captured digital aerial images are summarized in Table 1.

**Table 1** The specifications of the drone camera used and the digital aerial images captured in the present study (www.dji.com website, access date: March 1, 2021)

Camera manufacturer	DJI	Format	JPG
Camera model	FC6310	Color composite	RGB
Focal length	24 mm	Saturation	Normal mode
Size	5472×3448 Pixels	Sharpness	Normal mode
Volume	20 Mpixel	Contrast	Normal mode
Shutter speed	1/160 s	Drone speed	4 m/s
Horizontal resolution	72 dpi	Tilt sensor	Active
Vertical resolution	72 dpi	GNSS	GPS/GLONASS

The images were acquired on March 4, 2021 at 14:30 local time (UTC Time: 11:00 AM) and a total of 952 standard and checked images were captured to cover the study area. Fourteen ground control points (GCPs) were used to geo-reference the images and obtain their mosaic. In the selection of GCPs, issues such as the appropriate distance from each other, dispersion in the studied area along

with durability and appropriate visibility from different directions of image capture were considered. In order to avoid some errors, including stretching during imaging, a speed of about 4 m/s was used to automatically guide the UAV (Tu *et al.* 2020).

**Image preprocessing**

The captured images were examined separately in order to remove them from the work process if they were blurred, tilted more than allowed, or had a strong influence of sunlight. A three-dimensional model was derived by the remaining images using the structure from motion (SfM: Structure from motion) algorithm (Wallace *et al.* 2016; Sangjan *et al.* 2022) in Python. In the next step, the point cloud was prepared in high density mode (1.27 points per square centimeter). Median filter was used on the dense point cloud to reduce noise so as not to cause disturbances or errors in processing (Deluzet *et al.* 2022).

**Tree height estimation**

Three heights were estimated for each tree in addition to the height measured in the field, i.e., the height from CHM ( $H_{CHM}$ ), the height from the shadow length without slope correction ( $H_{Shad\_Uncorr}$ ) and the height from the shadow length after slope correction ( $H_{Shad\_Corr}$ ). The  $H_{CHM}$ ,  $H_{Shad\_Uncorr}$  and  $H_{Shad\_Corr}$  were compared with the heights measured in field.

In order to estimate the  $H_{CHM}$ , the digital surface model (DSM) and digital terrain model (DTM) of the study area were constructed using Inverse Distance Weighting (IDW) interpolation applied on the filtered point clouds (Pádua *et al.* 2019). Then CHM (Eq. 1) was with Ground Sampling Distance (GSD) of 2 cm as

$$CHM=DSM-DTM \tag{1}$$

The Marker-Controlled Watershed (MCW) algorithm was used to segment the CHM on which the heights of 151 pine trees were identified (Hernandez et al. 2016) using Python. The MCW is a non-linear algorithm that is mainly used for segmentation of CHMs in the literature (Huang et al., 2018). First, the top of the crowns of pine trees in the study area was determined by using a local maximum filter (Local maximum: LM). Since the control points were the crown tops of pine trees, the area marked around each point is a decreasing gradient and represents the area of the tree crown (Azizi & Miraki 2022). The crown tops of the pine trees detected with the LM filter on the CHM were used to determine the height of each tree.

With the continuous movement of the earth around the sun, the shadow locations change continuously, i.e. it is not possible to instantly measure the shadows of the entire area on UAV images, especially for very large areas. Trees with the shortest flight time were selected, in other words, the flight path was designed to be longer (Liu et al. 2017). For effective extraction of tree canopies on the UAV imagery, the  $VI_{green}$  index (Eq. 2) was used (Costa et al. 2020).

$$VI_{green} = (\text{green-red}) / (\text{green+red}) \quad (2)$$

In the next step, multiscale segmentation was performed on the image of  $VI_{green}$  index. In the segmentation process, according to the shape of the shadow of the pine trees and the conditions of the study area; appropriate coefficients for optimal segmentation parameters were selected by trial and error (Scale Parameter=30, Shape=0.1, Compactness=0.4 per pixel unit) and 0.33 was used as the threshold for shadow detection. The bounding box surrounded each shadow segment was obtained for each tree shadow (Vélez et al. 2022b). By calculating the distance from the top of the crown shadow on the ground to the top of the crown of the pine trees (identified with the LM filter on the CHM) according to the bounding box enclosing each tree shadow, the shadow length (D) was obtained for each tree.

The general principles of calculating the second height for each tree (H) using the shadow length is the product of the shadow length and the tangent of the solar altitude angle (Solar Altitude:  $\lambda$ ) (Eq. 3) (Safonova et al. 2021). According to the location of the study area and the date and time of imaging, the value of the elevation angle of the sun was  $32.8^\circ$  (<https://www.suncalc.org>).

$$H = D \times \tan \lambda \quad (3)$$

The surface of the earth often has a diverse topography. This diversity in the shape of the earth is not the same in all locations (Ozdemir2008). Therefore, considering the spatial location of a tree individual, it might have three types of shadows. In the first case, the shadow is placed on a positive (uphill) slope (AB in Fig. 2a), which means the length of the shadow is less than usual (compared to the ground with a zero degree slope) (AC in Fig. 2a). In the second case, the length of the shadow is placed on a ground with zero slope (AB in Fig. 2b). Although this condition happens very rarely, it is considered as one of the most important conditions because it is the geometric and measurement basis for other conditions. In the third case, the shadow is formed on the negative (downward) slope (AB in Fig. 2c). In this case, the length of the shadow is longer than usual (ground with zero degree slope) (AG Fig. 2c). Correcting the slope in the first and third cases can bring the shadow length closer to the real value of the shadow on the ground with zero slope, and the height of the tree obtained based on the corrected shadow length will be closer to the real value.

In this study, the height difference between the center of each tree (the same tip of the crown of the trees identified with the LM filter on CHM, A in Fig. 2) and the shadow tip (B in Fig. 2) on DTM were used. If this height difference was negative, Fig. 2a and if this height difference was positive, Fig. 2c were considered. According to trigonometric relationships, two methods for determining the

exact length of the shadow were proposed here, which are summarized in Table 2. According to the suggested relationships in Table 2, the third

height was estimated for a and c in Fig. 2. The flowchart of present study was provided in Fig. 3.

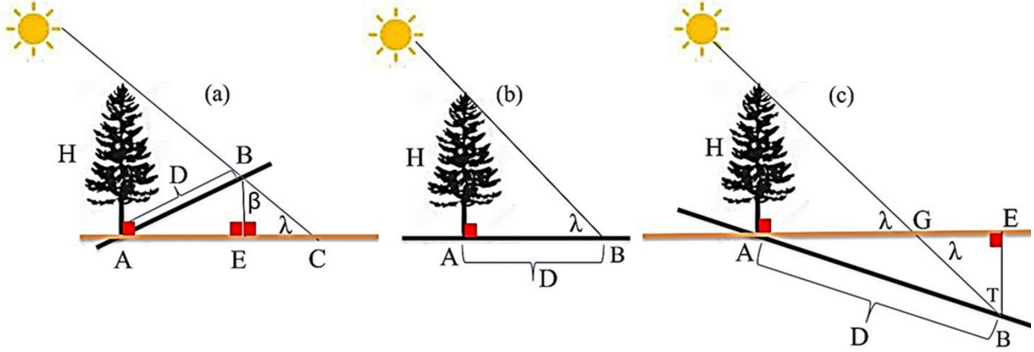


**Figure 2** Three states of tree shadows on the ground: positive slope (uphill) (a), zero slope (hypothetical state) (b), negative slope (downhill) (c). H is the height of the tree, D (AB) is the length of the formed shadow, BE is the height difference between the tip of the shadow and the base line.

**Table 2** Proposed method for estimating height with corrected shadow length based on trigonometric relationships

$\beta = 180^\circ - (\lambda + 90^\circ)$	
$EC = (\sin \beta \times BE) / \sin \lambda$	
$AE = \sqrt{D^2 - EB^2}$	Fig. 2a
$AC = AE + EC$	
$H = \tan \lambda \times AC$	
$H = \tan \lambda \times D$	Fig. 2b
$T = 180^\circ - (\lambda + 90^\circ)$	Fig. 2c
$GE = (\sin T \times BE) / \sin \lambda$	
$AE = \sqrt{D^2 - EB^2}$	
$AG = AE - GE$	
$H = \tan \lambda \times AG$	

### Assessment of accuracy and precision

The accuracy of the heights of pine trees estimated by the shadow length on the UAV RGB images and cloud points was investigated by a suitable statistical test to compare estimated values with the true values. First, the normality of the data was checked with the Kolmogorov-Smirnov test, and if it was normal, the paired t-test was used, and otherwise, the Wilcoxon test was used. Also, the one-to-one graph of real and estimated values in two methods and their correlation coefficient were evaluated. Then, the one-to-one graph and the coefficient of determination of the fitted line were evaluated. The accuracy of the results were evaluated by

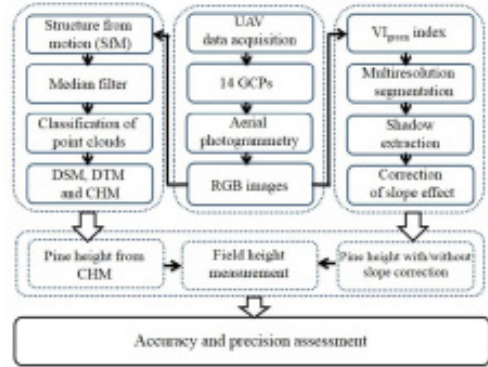


**Figure 3** Flowchart of the present study.

Relative Root Mean Squared Error (RRMSE) (Eq. 4), Model Efficiency (ME) (Eq. 5) and Bias Score (BS) (Eq. 6).

$$RRMSE(100) = \frac{\sqrt{\frac{1}{n} \sum (y_i - \hat{y}_i)^2}}{\sqrt{\sum (\hat{y}_i)^2}} \times 100 \quad (4)$$

$$ME = \frac{|\sum (y_i - \hat{y}_i)^2 - \sum (\hat{y}_i - y_i)^2|}{\sum (y_i - \hat{y}_i)^2} \quad (5)$$

$$BS = \frac{\sum (y_i - \hat{y}_i)^2}{\sum (\hat{y}_i - y_i)^2} \quad (6)$$

where  $y_i$  is the true height,  $\hat{y}_i$  is the estimated height,  $n$  is the number of samples and  $\bar{y}$  is the average of the real data.

In equation 4, the closer the RRMSE value is to zero, the more efficient the method is. In Eq. 5, the value of  $ME=1$  indicates the good efficiency of the method. On the other hand, a negative value means rejecting the effectiveness of the method. In Eq. 6, a BS value greater than one indicates a higher estimate than the actual value, and if this parameter is less than one, it indicates a lower estimate of the height compared to its actual value (Hao et al. 2021).

## Results

Fig. 4 shows that the distribution of DBH ( $p=0.738$ ) and height ( $p=0.416$ ) of the sample trees were not significantly different from the normal distribution. Although the only parameter needed in this study was the height of pine trees, but the distribution of DBH in addition to height indicated that sample trees were well distributed in all size classes. The size distribution of the sample trees, ranging from 0.5 m to 11.2 m in height (average: 6.3 m, coefficient of variation: 38.6%), and from 1 cm to 62 cm in diameter at breast height (DBH) (average: 36.5 cm, coefficient of variation: 29.9%), illustrates that the sample trees were not confined to a single size class. Instead, they were well-distributed across a broad range, encompassing both small and large trees grown

in the study area (Table 3).

Fig. 5 shows the map of the crown and shadow of pine trees on the UAV RGB images. Thanks to very high spatial resolution of the UAV orthomosaic (i.e., 2 cm), the crowns and shadows of all tree individuals were precisely delineated within the study site. The crowns and shadows of three sample trees are illustrated in Fig. 5 for visual interpretation of the results. In order to determine the exact length of the crown shadows, the bounding box enclosing each shadow was obtained and the length of the rectangle plus the distance from the center of the crown to its lower width was considered as the length of the shadow (Fig. 5). In addition, the difference in the height of the center of the tree crown and the top of the shadow was the basis of the slope correction of shadow length as explained in Fig. 2.

Table 3 shows the results of estimating the height of 151 pine trees by three methods. Comparing the estimated height with the in-situ height of the trees showed that the amount of height estimated by corrected shadow length ( $H_{\text{Shad\_Corr}}$ ) was closer to the height obtained from the field measurement, which was considered as the true values, compared to the estimated height with the uncorrected shadow length ( $H_{\text{Shad\_Uncorr}}$ ). Moreover, the statistical test confirmed that there was no significant difference between the estimated heights with corrected shadow length and the true

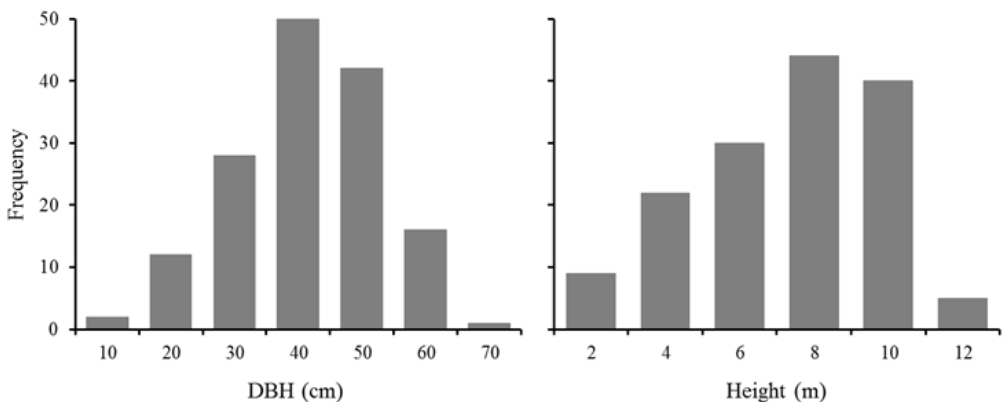
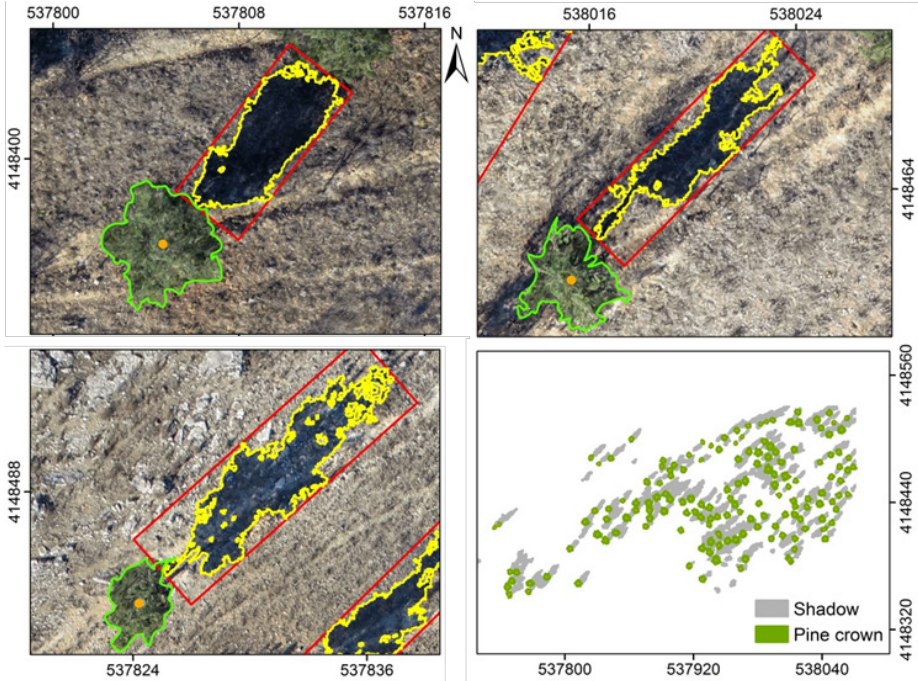


Figure 4 Frequency distribution of height (right) and diameter at breast (left) of 151 pine trees in the study area.



**Figure 5** Crown and shadow map of 151 pine trees in the study area, as an example, three tree crowns and their shadows are shown on the orthomosaic of the area. The red rectangle is the bounding box surrounding each tree shadow, which was used to measure the length of the shadow.

heights ( $p=0.298$ ). However, this difference was significant in the case of estimated height with uncorrected shadow length ( $H_{\text{Shad\_Uncorr}}$ ) ( $p<0.05$ ). Additionally, the  $H_{\text{CHM}}$  was not significantly different from the true height values ( $p=0.478$ ).

In addition to accuracy assessment of the results, the precision evaluation also showed that the height estimated with the corrected shadow length showed less RRMSE (5.6% and 8.2% respectively), BS (0.41% and 0.33% respectively) and ME (respectively 0.74 and 0.68) compared to the height estimated by uncorrected shadow length. Furthermore, the HCHM had less RRMSE (4.2%), BS (0.01) and higher ME (0.98) compared to the  $H_{\text{Shad\_Corr}}$ . In general, the results showed that based on the mentioned indices, the  $H_{\text{Shad\_Corr}}$  exhibited higher accuracy and precision compared to the height obtained without correcting the slope of the shadow length. However, the accuracy of the  $H_{\text{CHM}}$  was higher than that of obtained from the UAV RGB images.

The results of Kolmogorov-Smirnov test showed that the  $H_{\text{Shad\_Corr}}$  ( $p=0.519$ ),  $H_{\text{Shad\_Uncorr}}$  ( $p=0.661$ ) and the  $H_{\text{CHM}}$  ( $p=0.351$ ) had a normal distribution. Pearson's correlation coefficient also showed a significant correlation (at the 5% level) between the true height of the trees with the  $H_{\text{Shad\_Uncorr}}$  (0.84,  $p<0.05$ ),  $H_{\text{Shad\_Corr}}$  (0.96,  $p<0.05$ ) and  $H_{\text{CHM}}$  (0.99,  $p>0.05$ ). Fig. 6 illustrates the correlations of true height values with  $H_{\text{Shad\_Uncorr}}$ ,  $H_{\text{Shad\_Corr}}$  and  $H_{\text{CHM}}$ .

## Discussion

In the present study, we used UAV RGB data to improve height estimation of pine trees within a mountainous plantation forest. Our main objective included estimation of tree height based on shadow length that the effect of slope on it was corrected. We compared the height obtained from in-situ measurement with the height estimated on UAV orthomosaic using shadow length and UAV-based CHM in order to evaluate the efficiency of the proposed approach for height estimation of trees on RGB

images. In general, our findings agree with the rich literature supporting the application of UAV datasets in estimation of tree quantitative attributes such height (Paneque-Gálvez et al. 2014, Gülci 2019, Safonova et al. 2021). Several works have been focused on height estimation on UAV RGB imagery (Selim et al. 2020, Safonova et al. 2021), however, topographic characteristics of forest stands and their effects on shadow length of trees have less been considered in height estimation on remotely sensed VHR datasets. The present study can be considered a step forward in estimating tree height on UAV VHR imagery based on shadow length.

In line with previous researches (Birdal et al. 2017, Lawrence et al. 2022), our study considered tree samples with an appropriate range of size. As shown in Fig. 3, the selected pine trees within the study area followed normal distribution indicating that the trees were not limited to a specific size class. Therefore, the findings may be more reliable comparing to

studies that focus on samples with limited size range. As reported by Abdullahzadeh et al. (2003), size of pine trees planted in Lavizan Park, Tehran, Iran, varied from height of 1.7 m (with DBH of 5 cm) to a height of 12.5 m (with DBH of 34 cm). Additionally, Kiani and Madadi (2021) found that pine trees in Sorkhehesar Park exhibited height of 2.5 m (with DBH of 5.7 cm) to 18.7 m (with DBH of 41.4 cm). Our results indicated that height (DBH) of pine trees within Pardisan Park ranged from 0.5 m (1.0 cm) to 11.2 m (62.0 cm) indicating the establishment of young trees and higher growth rate considering the DBH. However, future studies may explore the probable reasons of such observations within the parks.

We could accurately delineate shadow of each tree individual on the UAV orthomosaic due to very high spatial resolution (i.e., 2 cm) of the data. Furthermore, the spatial location of trees and the type of slope they are located were identified because of access to the DTM of the

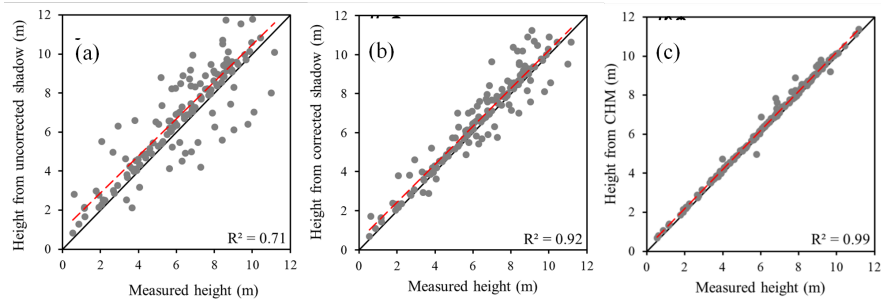


**Figure 6** One-to-one diagram of true height of 151 pine trees with estimated height from uncorrected shadow (a), corrected shadow (b) and crown height model (CHM) (c). R<sup>2</sup> is the coefficient of explanation of the fitted line (red dashed line) to the data.

**Table 3** A summary of the statistical characteristics of the height of 151 pine trees estimated on UAV data (tmeasure unit: meters).

Parameter	Minimum	Maximum	Mean	Standard deviation	Coefficient of variation (%)
True height	0.5	11.2	6.3	2.4	38.6
Height from uncorrected shadow	0.8	13.4	7.0*	2.7	39.2
Height from corrected shadow	0.7	12.4	6.6 <sup>ns</sup>	2.6	38.0
Height from CHM	0.7	11.2	6.5 <sup>ns</sup>	2.5	37.6

study site. Therefore, this study could test the hypothesis primarily made, i.e., the effect of slope correction of height estimation of trees using shadow length. As previous studies emphasized (Selim *et al.* 2020, Safonova *et al.* 2021), the use of shadow length to determine the height of trees on aerial images can only be used in ecosystems where trees are far apart. The approach may be also considered in open plantation forests (such as the study area of the current research) and arid and semi-arid woodlands, e.g., the Zagros forests, western Iran (Rezayan & Erfanifard, 2016). This is worth mentioning that the methodology is applicable to forest stands with specific conditions and need RGB images and DTM with very high spatial resolutions.

In our study, the crowns and shadows of trees were mapped using segmentation method on the VIgreen index image with high accuracy. However, deep learning algorithms (such as convolutional neural network or CNN) (Safonova *et al.* 2021) may also be considered in future studies to identify tree crowns and shadows. Moreover, the MCW algorithm was used for CHM segmentation, the efficiency of which has been confirmed in previous studies (Erfanifard & Kraszewski 2021; Chen *et al.* 2021). The use of MCW in the present study is in accordance with previous studies. The efficiency of the algorithm in identifying pine trees has also been confirmed in previous studies (Kim *et al.* 2010, McMahon 2019). It should be noted that the results of the present study in height estimation on CHM are in line with the achievements of Castilla *et al.* (2020) and Li *et al.* (2022), who pointed out that the segmentation of UAV-based CHM is efficient in estimating the height of pine trees (*Pinus banksiana*) specially for young planted individuals.

In a recent study by Rezayan and Erfanifard (2016), the height of 162 Persian oak trees located in the Zagros semi-arid woodlands, western Iran, were calculated using tree shadow. The correlation coefficient of estimated values

and the true in-situ values was 0.85, which was less compared to the correlation coefficient between the true height and  $H_{\text{Shad\_Corr}}$  (0.96) in the present study. The woodlands are mostly distributed on mountainous areas; therefore, application of shadow length with slope correction may improve height estimation. The hypothesis may be addressed in futures works. The proposed approach for height estimation of pine trees on UAV RGB imagery is important. First, it is not always possible to prepare dense point clouds and accurate CHM in some VHR data, despite access to CHM from UAV data. Second, some researchers prefer to use shadow length on UAV color images to estimate tree height (Selim *et al.* 2020, Safonova *et al.* 2021, Vélez *et al.* 2022b). Therefore, it seems necessary to develop reliable methods in addition to height estimation methods on CHM.

In previous studies (Selim *et al.* 2020, Safonova *et al.* 2021), height of trees were estimated using the length of the shadow on UAV RGB images. As mentioned earlier, the effect of slope on shadow length was not necessary to be considered in previous studies since most of the study sites in flat agricultural plots were almost plain with no or little slope changes. However, there are natural and man-made forests located on steep slopes of mountainous areas. Therefore, our findings provides deeper insights for managers of plantation forests wishing to integrate remotely sensed datasets collected by UAV into their management activities and strategies. First, there are significant achievements to be gained from the implementation of UAV datasets into collection of information necessary in sustainable management. The estimation of tree biophysical properties such as height and crown attributes is significantly time efficient compared to field measurements. Second, view from top provided by VHR remotely sensed data provide opportunities to estimate some properties with higher accuracies compared to in-situ measurements. Height, for instance, is

one of the properties hard to measure especially for old large trees. Third, as the heights obtained from field and UAV were not significantly different, these results suggest the efficiency of the proposed approach in this study. Finally, there are some points highlighted through this study relating to height estimation in UAV-based CHM and image segmentation. For example, tree heights estimated from the CHM were closely related to field measurements indicating the reliability of the approach as shown by previous works (Paneque-Gálvez et al. 2014, Gülci 2019). In line with the findings of the present study, Krause et al. (2019), for example, estimated the height of 251 planted pine trees (*Pinus sylvestris*) on UAV-based CHM with a correlation coefficient of 0.99. According to these results, it is possible to emphasize the efficiency of CHM in estimating height of pine trees and recommend the approach for estimating height of trees in areas where CHM is available or shadow length cannot be recognized because of high tree density.

## Conclusions

The present study aimed to estimate height of pine single trees based on slope corrected shadow length on UAV imagery. Estimation of tree height using shadow length has been widely applied in the literature; however, less attention has been paid to the effect of slope on the shadow length in mountainous areas that may influence the accuracy and precision of height estimation. Therefore, the present study proposed a novel approach to estimate the height of single pine trees in a plantation forest using shadow length on UAV RGB images. In general, the findings of the research showed that correction of slope in determination of shadow length on UAV RGB imagery significantly improved height estimation. The estimated heights with the corrected shadow length had no significant difference from the true values ( $p=0.298$ ) with more accuracy than the estimated height without correcting the effect of slope on the shadow length. However, the estimated height with corrected shadow

length was less accurate than the estimated height on CHM (RRMSE 5.6% and 4.2%, respectively). Finally, it can be concluded that it is necessary to correct the slope effect in estimating height of trees using the shadow length in mountainous areas. Additionally, it is acknowledged that if applicable, CHM is more reliable than UAV RGB images for estimating height of single trees.

## Acknowledgment

The authors are grateful to the General Department of Environmental Protection, especially Dr. Mehdi Elahpour and Dr. Iskandar Gardmardi, the environmentalists of Pardisan Park and Ms. Mozghan Dehghani. Also, a part of the costs of this research was provided by the Iran National Science Foundation (INSF) (Project number 4003393).

## References

- Abdullahzadeh B., Tabari M., Sagheb Talebi Kh., & Zobeiri, M. 2003. Response of diameter and height of *Pinus eldarica* Medw. to slope and aspect variations in Lavizan Forest Park. *Pajouhesh-va-Sazandegi*, 16(3), 30-35. (In Persian).
- Apostol B., Lorent A., Petrila M., Gancz V., & Badea O. 2016. Height extraction and stand volume estimation based on fusion airborne LiDAR data and terrestrial measurements for a Norway spruce [*Picea abies* (L.) Karst.] test site in Romania. *Notulae Botanicae Horti Agrobotanici Cluj-Napoca*, 44(1), 313-323. <https://doi.org/10.15835/NBHA44110155>.
- Azizi Z., & Miraki M. 2022. Individual urban trees detection based on point clouds derived from UAV-RGB imagery and local maxima algorithm, a case study of Fateh Garden, Iran. *Environment, Development and Sustainability*, <https://doi.org/10.1007/s10668-022-02820-7>
- Barbosa R.I., Ramirez-Narváez P.N., Fearnside, P.M., Villacorta C.D.A., Carvalho L.C., & da S. 2019. Allometric models to estimate tree height in northern Amazonian ecotone forests. *Acta Amazonica*, 49, 81-90.
- Birdal A.C., Avdan U., & Türk T. 2017. Estimating tree heights with images from an unmanned aerial vehicle. *Geomatics, Natural Hazards and Risk*, 8(2), 1144-1156. <https://doi.org/10.1080/19475705.2017.1300608>.
- Bragg D.C. 2014. Accurately measuring the height of (real) forest trees. *Journal of Forestry*, 112(1), 51-54. <https://doi.org/10.5849/jof.13-065>.
- Castilla G., Filiatrault M., McDermid G. J., & Gartrell, M. 2020. Estimating individual conifer seedling height using drone-based image point clouds. *Forests*, 11(9), 924. <https://doi.org/10.3390/f11090924>.
- Chadwick A.J., Goodbody T.R., Coops N.C., Hervieux A., Bater C.W., Martens L.A., & Roeser, D. 2020. Automatic delineation and height measurement of

- regenerating conifer crowns under leaf-off conditions using UAV imagery. *Remote Sensing*, 12(24), 4104. <https://doi.org/10.3390/rs12244104>.
- Chen X., Lee R.M., Dwivedi D., Son K., Fang Y., Zhang X., & Scheibe T.D. 2021. Integrating field observations and process-based modeling to predict watershed water quality under environmental perturbations. *Journal of Hydrology*, 602, 125762. <https://doi.org/10.1016/j.jhydrol.2020.125762>.
- Costa L., Nunes L., & Ampatzidis Y. 2020. A new visible band index (vNDVI) for estimating NDVI values on RGB images utilizing genetic algorithms. *Computers and Electronics in Agriculture*, 172, 105334. <https://doi.org/10.1016/j.compag.2020.105334>.
- Dandois J.P., Olano M., & Ellis E.C. 2015. Optimal altitude, overlap, and weather conditions for computer vision UAV estimates of forest structure. *Remote Sensing*, 7(10), 13895-13920. <https://doi.org/10.3390/rs71013895>.
- Deluzet M., Erudel T., Briottet X., Sheeren D., & Fabre S. 2022. Individual tree crown delineation method based on multi-criteria graph using geometric and spectral information: application to several temperate forest sites. *Remote Sensing*, 14(5), 1083. <https://doi.org/10.3390/rs14051083>.
- Dempewolf J., Nagol J., Hein S., Thiel C., & Zimmermann R. 2017. Measurement of within-season tree height growth in a mixed forest stand using UAV imagery. *Forests*, 8(7), 231. <https://doi.org/10.3390/f8070231>.
- Erfanifard Y., Chenari A., Dehghani M., & Amiraslani F. 2019. Effect of spatial resolution of UAV aerial images on height estimation of wild pistachio (*Pistacia atlantica* Desf.) trees. *Iranian Journal of Forest and Poplar Research*, 27(2), 169-181. (In Persian).
- Erfanifard Y., & Kraszewski B. 2021. Estimation of qualitative and quantitative characteristics of *Pistacia atlantica* Desf. and *Amygdalus* spp. in of UAV point clouds. *Iranian Journal of Forest and Poplar Research*, 29(1), 13-26. (In Persian)
- Food and Agricultural Organization (FAO) 2020. *Global Forest Resources Assessment 2020*, 186 p.
- Grote R., Gessler A., Hommel R., Poschenrieder W., & Priesack E. 2016. Importance of tree height and social position for drought-related stress on tree growth and mortality. *Trees*, 30(5), 1467-1482. <https://doi.org/10.1007/s00468-016-1446-x>.
- Gülci S. 2019. The determination of some stand parameters using SfM-based spatial 3D point cloud in forestry studies: An analysis of data production in pure coniferous young forest stands. *Environmental monitoring and assessment*, 191(8), 1-17. <https://doi.org/10.1007/s10661-019-7628-4>.
- Guo Y., Chen S., Wu Z., Wang S., Robin Bryant C., Senthilnath J., & Fu Y.H. 2021. Integrating spectral and textural information for monitoring the growth of pear trees using optical images from the UAV platform. *Remote Sensing*, 13(9), 1795. <https://doi.org/10.3390/rs13091795>.
- Gyawali A., Aalto M., Peuhkurinen J., Villikka M., & Ranta T. 2022. Comparison of individual tree height estimated from LiDAR and digital aerial photogrammetry in young forests. *Sustainability*, 14(7), 3720. <https://doi.org/10.3390/su14073720>.
- Hao Z., Lin L., Post C. J., Jiang Y., Li M., Wei N., & Liu J. 2021. Assessing tree height and density of a young forest using a consumer unmanned aerial vehicle (UAV). *New Forests*, 52(5), 843-862. <https://doi.org/10.1007/s11056-020-09827-w>.
- Hartley R.J., Leonardo E.M., Massam P., Watt M.S., Estarija H.J., Wright L., & Pearse G.D. 2020. An assessment of high-density UAV point clouds for the measurement of young forestry trials. *Remote Sensing*, 12(24), 4039. <https://doi.org/10.3390/rs12244039>.
- Hernandez J.G., Gonzalez-Ferreiro E., Sarmento A., Silva J., Nunes A., Correia A. C., & Diaz-Varela R. 2016. Using high resolution UAV imagery to estimate tree variables in *Pinus pinea* plantation in Portugal. *Forest Systems*, 25(2), eSC09-eSC09. <https://doi.org/10.5424/fs/2016252-08895>.
- Huang H., Li X., & Chen C. 2018. Individual tree crown detection and delineation from very-high-resolution UAV images based on bias field and marker-controlled watershed segmentation algorithms. *IEEE Journal of selected topics in applied earth observations and remote sensing*, 11(7), 2253-2262. <https://doi.org/10.1109/JSTARS.2018.2830410>.
- Kargar M.R., & Sohrobi H. 2019. Using canopy height model derived from UAV images to tree height estimation in Sisanang forest. *Journal of RS and GIS for Natural Resources*, 10(3), 106-119. <http://dorl.net/dor/20.1001.1.26767082.1398.10.3.7.8>.
- Kiani B. & Madadi R. 2021. Assessing the risk of windthrow for Eldar pine trees in Sorkhe-Hesar forest park. *Wood and Forest Science and Technology*, 28(1), 37-52. (In Persian).
- Kim S.R., Kwak D.A., Olee W.K., Son Y., Bae S.W., Kim C., & Yoo S. 2010. Estimation of carbon storage based on individual tree detection in *Pinus densiflora* stands using a fusion of aerial photography and LiDAR data. *Science China Life Sciences*, 53(7), 885-897. <https://doi.org/10.1007/s11427-010-4017-1>.
- Kislov D.E., & Korznikov K.A. 2020. Automatic windthrow detection using very-high-resolution satellite imagery and deep learning. *Remote Sensing*, 12(7), 1145. <https://doi.org/10.3390/rs12071145>.
- Krause S., Sanders T.G., Mund J.P. & Greve K. 2019. UAV-based photogrammetric tree height measurement for intensive forest monitoring. *Remote sensing*, 11(7), 758. <https://doi.org/10.3390/rs11070758>.
- Lawrence B. 2022. Classifying forest structure of red-cockaded woodpecker habitat using structure from motion elevation data de-Rived from sUAS imagery. *Drones*, 6(1), 26. <https://doi.org/10.3390/drones6010026>.
- Li L., Mu X., Chianucci F., Qi J., Jiang J., Zhou J., & Liu S. 2022. Ultrahigh-resolution boreal forest canopy mapping: Combining UAV imagery and photogrammetric point clouds in a deep-learning-based approach. *International Journal of Applied Earth Observation and Geoinformation*, 107, 102686. <https://doi.org/10.1016/j.jag.2022.102686>.
- Liu X., Hou Z., Shi Z., Bo Y., & Cheng, J. 2017. A shadow identification method using vegetation indices derived from hyperspectral data. *International Journal of Remote Sensing*, 38(19), 5357-5373. <http://dx.doi.org/10.1080/01431161.2017.1338785>.

- McMahon C.A. 2019. Remote sensing pipeline for tree segmentation and classification in a mixed softwood and hardwood system. *PeerJ*, 6, e5837. <https://doi.org/10.7717/peerj.5837>.
- Moe K.T., Owari T., Furuya N., & Hiroshima T. 2020. Comparing individual tree height information derived from field surveys, LiDAR and UAV-DAP for high-value timber species in Northern Japan. *Forests*, 11(2), 223. <https://doi.org/10.3390/f11020223>.
- Navarro A., Young M., Allan B., Carnell P., Macreadie P., & Ierodiakonou D. 2020. The application of Unmanned Aerial Vehicles (UAVs) to estimate above-ground biomass of mangrove ecosystems. *Remote Sensing of Environment*, 242, 111747. <https://doi.org/10.1016/j.rse.2020.111747>.
- Onishi M., & Ise T. 2021. Explainable identification and mapping of trees using UAV RGB image and deep learning. *Scientific Reports*, 11(1), 1-15. <https://doi.org/10.1038/s41598-020-79653-9>.
- Onishi M., Watanabe S., Nakashima T., & Ise T. 2022. Practicality and robustness of tree species identification using UAV RGB image and deep learning in temperate forest in Japan. *Remote Sensing*, 14(7), 1710. <https://doi.org/10.3390/rs14071710>.
- Ozdemir I. 2008. Estimating stem volume by tree crown area and tree shadow area extracted from pan-sharpened Quickbird imagery in open Crimean juniper forests. *International Journal of Remote Sensing*, 29(19), 5643-5655. <https://doi.org/10.1080/01431160802082155>.
- Pádua L., Guimarães N., Adão T., Marques P., Peres E., Sousa A., & Sousa J.J. 2019. Classification of an agrosilvopastoral system using RGB Imagery from an unmanned aerial vehicle. In *EPIA Conference on Artificial Intelligence*, 248-257. Springer, Cham. [https://doi.org/10.1007/978-3-030-30241-2\\_22](https://doi.org/10.1007/978-3-030-30241-2_22).
- Paneque-Gálvez J., McCall M.K., Napoletano B.M., Wich S.A., & Koh L.P. 2014. Small drones for community-based forest monitoring: An assessment of their feasibility and potential in tropical areas. *Forests*, 5(6), 1481-1507. <https://doi.org/10.3390/f5061481>.
- Puliti S., Breidenbach J., & Astrup R. 2020. Estimation of forest growing stock volume with UAV laser scanning data: can it be done without field data? *Remote Sensing*, 12(8), 1245. <https://doi.org/10.3390/rs12081245>.
- Rezayan F., & Erfanfard Y. 2016. Estimating biophysical parameters of Persian oak coppice trees using UltraCam-D airborne imagery in Zagros semi-arid woodlands. *Journal of Arid Environments*, 133, 10-18. <https://doi.org/10.1016/j.jaridenv.2016.05.002>.
- Safonova A., Guirado E., Maglinets Y., Alcaraz-Segura D., Tabik, S. 2021. Olive tree biovolume from UAV multi-resolution image segmentation with Mask R-CNN. *Sensors*, 21, 1617. <https://doi.org/10.3390/s21051617>.
- Sangjan W., McGee R. J., & Sankaran S. 2022. Optimization of UAV-based imaging and image processing orthomosaic and point cloud approaches for estimating biomass in a forage crop. *Remote Sensing*, 14(10), 2396. <https://doi.org/10.3390/rs14102396>.
- Seifert E., Seifert S., Vogt H., Drew D., Van Aardt J., Kunneke A., & Seifert T. 2019. Influence of drone altitude, image overlap, and optical sensor resolution on multi-view reconstruction of forest images. *Remote sensing*, 11(10), 1252. <https://doi.org/10.3390/rs11101252>.
- Selim S., Kalaycı M., & Kılıçık A. 2020. Obtaining height information using a 2-D top view UAV image with the help of spherical astronomy. *Journal of Indian Society of Remote Sensing*, 48, 1083-1090. <https://doi.org/10.1007/s12524-020-01139-y>.
- Surový P., Almeida Ribeiro N., & Panagiotidis D. 2018. Estimation of positions and heights from UAV-sensed imagery in tree plantations in agrosilvopastoral systems. *International Journal of Remote Sensing*, 39(14), 4786-4800.
- Suzuki K., Ishii K., Sakurai S., & Sasaki S. (Eds.). 2006. *Plantation technology in tropical forest science* (pp. 53-66). Tokyo: Springer.
- Thu Moe K., & Owari T. 2020. Predicting individual tree growth of high-value timber species in mixed conifer-broadleaf forests in northern Japan using long-term forest measurement data. *Journal of Forest Research*, 25(4), 242-249. <https://doi.org/10.1080/13416979.2020.1790095>.
- Tian J., Dai T., Li H., Liao C., Teng W., Hu Q., & Xu Y. 2019. A novel tree height extraction approach for individual trees by combining TLS and UAV image-based point cloud integration. *Forests*, 10(7), 537. <https://doi.org/10.3390/f10070537>.
- Tu Y.H., Phinn S., Johansen K., Robson A., & Wu D. 2020. Optimising drone flight planning for measuring horticultural tree crop structure. *ISPRS Journal of Photogrammetry and Remote Sensing*, 160, 83-96. <https://doi.org/10.1016/j.isprsjprs.2019.12.006>.
- Vélez S., Vacas R., Martín H., Ruano-Rosa D., & Álvarez S. 2022a. High-resolution UAV RGB imagery dataset for precision agriculture and 3D photogrammetric reconstruction captured over a pistachio orchard (*Pistacia vera* L.) in Spain. *Data*, 7(11), 157. <https://doi.org/10.3390/data7110157>.
- Vélez S., Vacas R., Martín H., Ruano-Rosa D., & Álvarez S. 2022b. A novel technique using planar area and ground shadows calculated from UAV RGB imagery to estimate pistachio tree (*Pistacia vera* L.) canopy volume. *Remote Sensing*, 14(23), 6006. <https://doi.org/10.3390/rs14236006>.
- Wallace L., Lucieer A., Malenovsky Z., Turner D., & Vopěnka P. 2016. Assessment of forest structure using two UAV techniques: A comparison of airborne laser scanning and structure from motion (SfM) point clouds. *Forests*, 7(3), 62. <https://doi.org/10.3390/f7030062>.
- Yao Q., Wang J., Zhang J., & Xiong N. 2022. Error analysis of measuring the diameter, tree height, and volume of standing tree using electronic theodolite. *Sustainability*, 14(12), 6950. <https://doi.org/10.3390/su14126950>.
- Zhou X., & Zhang X. 2020. Individual tree parameters estimation for plantation forests based on UAV oblique photography. *IEEE Access*, 8, 96184-96198.
- Zhu Y., Jeon S., Sung H., Kim Y., Park C., Cha S., & Lee W.K. 2020. Developing UAV-based forest spatial information and evaluation technology for efficient forest management. *Sustainability*, 12(23), 10150. <https://doi.org/10.3390/su122310150>.